



21st European Conference on Fracture, ECF21, 20-24 June 2016, Catania, Italy

Numerical simulation of fatigue crack growth in friction stir welded T joint made of Al 2024 T351 alloy

Abubakr Kredegh^a, Aleksandar Sedmak^a, Aleksandar Grbovic^a, Nenad Milosevic^a, Darko Danicic^b

^aFaculty of Mechanical Engineering, University of Belgrade, Swrbia,

^bRB Kolubara, EPS, Serbia

Abstract

The Extended Finite Element Method (xFEM) has been applied to simulate fatigue crack growth in an AA2024-T351 T welded joint, 5 mm thick, made by friction stir welding. The ABAQUS and Morfeo software has been used. Tensile fatigue loading (mean stress 10 MPa, stress ratio $R=0$) is applied to Tjoints with a configuration suitable for reinforced panels where both skin and the web (reinforcement or stiffener) is made of a high strength AA2024-T351. Crack is introduced in one edge of the skin base material. The properties of materials in the areas of joints and geometry measures of Tjoint are adopted from available experiments. Following numerical results are obtained: crack front coordinates (x , y , z) and stress intensity factors (K_I , K_{II} , K_{III} and K_{ef}) distribution along the crack tip, as well as the fatigue life estimation for every crack propagation step. The main objective of this research is to better understand fatigue behaviour of friction stir welded T joint of AA2024-T351.

© 2016, PROSTR (Procedia Structural Integrity) Hosting by Elsevier Ltd. All rights reserved.
Peer-review under responsibility of the Scientific Committee of ECF21.

Keywords: friction stir welding; aluminum alloys; fatigue crack growth; extended finite element method; fatigue life

1. Introduction

The large scale use of welding for joining of aerospace structures has long being inhibited by the difficulty of production of Al alloys welds with high fatigue strength, especially in the case of 2XXX and 7XXX series. These types of aluminum alloys are usually perceived as non-weldable due to limited porosity and microstructure during solidification in the fusion zone. There is also a substantial loss in the mechanical properties as related to the base material. The Welding Institute (TWI) came up with Friction Stir Welding (FSW) in 1991 as a process for joining Al alloys in the solid state, providing good mechanical properties and avoiding aforementioned problems, Thomas (1995). The concept behind FSW can be perceived as very simple, but still a bit complex when applied to produce T

joints. Different alternatives to produce T joints using FSW are shown in Figure 1, and more details are presented in Djurdjevic (2015), Zivkovic (2015) and Zivkovic (2015).

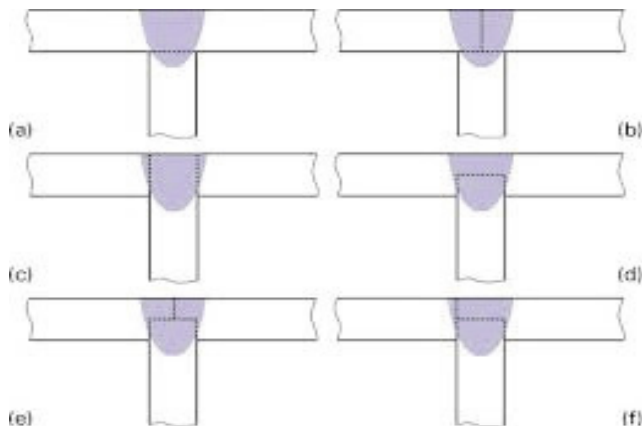


Figure 1. Different alternatives to produce T joints using FSW

(a) T- joint in two parts, (b) T- joint in three parts without penetration, (c) T- joint in three parts with complete penetration, (d) T- joint in two parts with partial penetration, (e) T- joint in three parts with partial penetration, (f) T- joint in three parts with partial penetration.

The T joint specimens were produced from two flat plates, 5 mm thick. Numerical simulation of the tensile test of T joints using the non-linear finite element code ABAQUS were performed, in order to improve the understanding of the behavior of this type of joint. ABAQUS software and Morfeo are used to display the results of the growth of cracks in FSW 2024-T351 welded joints in all regions. Tensile fatigue load stress is applies, with a ratio of the stress intensity $R = 0$ with maximum stress 10MPa. The properties of materials in the areas of joints and geometry measures of FSW joint are adopted from available experiments

2. Material properties in Friction Stir Welding (FSW)

This paper presents the analysis of the crack propagation in friction stir welded T joint of two plates (5 mm thick), made of aluminum alloy 2024-T351. Four different zone of welded joint are shown in figure 2. The mechanical properties of the materials are defined for each of these zones with values and are shown in Tables 1 and 2. The constant Paris law (C and m) are taken from Ali’s experiments same value for all zones, $C=2.02345 \cdot 10^{-10}$ cycles⁻¹, $m=2.94$, (Golestaneh, A. F, *Materials and Design* 2009, Golestaneh, A. F, *Suranaree Journal of Science and Technology* 2009, Zivojinović, D., 2011).

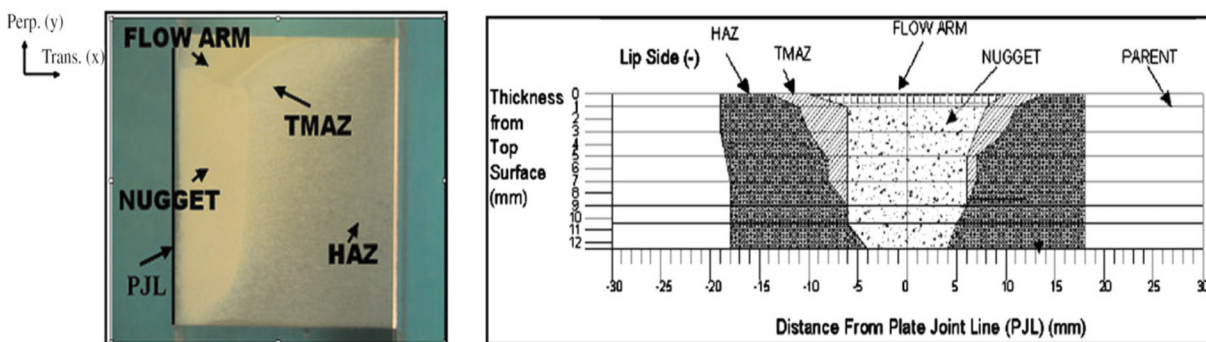


Fig. 2. The transverse cross section in as-welded FSW 2024-T351 Al Alloy T joint and the mapping of boundaries between macrostructural zones.

Table 1. Material properties in Friction Stir Welding of Al Alloy 2024-T351

Fsw regimes	PZ	HAZ	TMAZ	NZ
Young's modulus	68000	68000	68000	68000
Poisson's ratio	0.33	0.33	0.33	0.33
Yield stress (MPa)	370.00	484.00	272.00	350.00
Hardening constant	770.00	719.00	800.00	-
Hardening exponent	0.086	0.05546	0.1266	-
Hardness (Hv1)	132.00	167.00	118.00	142.00

Table 2. Stress-strain data of FSW zones

PZ		HAZ		TMAZ		NZ	
Stress (MPa)	Strain	Stress (MPa)	Strain	Stress (MPa)	Strain	Stress (MPa)	Strain
20	0.0003	25	0.0004	50.34	0.00070	30.43	0.00044
40	0.0006	35	0.0006	75.86	0.00123	51.30	0.00080
45	0.0009	58	0.00100	106.90	0.00160	69.56	0.00120
90	0.0014	83	0.00126	131.03	0.00200	91.30	0.00150
125	0.0021	95	0.00150	186.21	0.00310	130.43	0.00210
220	0.0034	130	0.00200	268.96	0.00450	186.95	0.00320
300	0.0050	175	0.00280	331.03	0.00570	286.96	0.00430
320	0.0058	280	0.00438			331.31	0.00550
440	0.0084	330	0.00558				
487	0.0120	480	0.00898				
		540	0.01166				

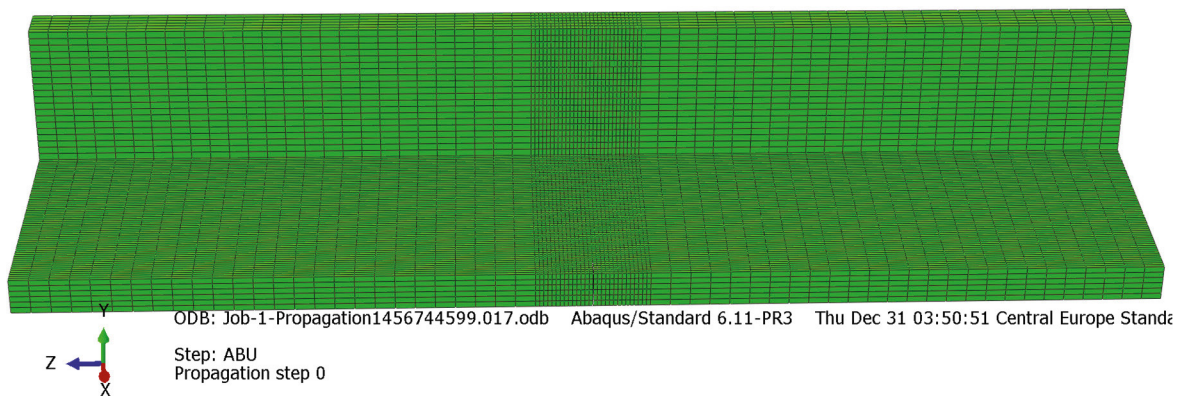


Fig. 3. The 3D Finite element Model of FSW compound.

3. Numerical model of Aluminum 2024-T351 T-joint

The structure of two friction stir welded joints consists of different stages for numerical simulation of crack growth within the structure:

1. Create 3D model (shape and dimensions), Fig. 3.

2. Defining the materials, mechanical properties for all different zones.
3. Introducing the initial crack within the structure, including its shape and location.
4. Introduce the loading including its intensity, type and location within the structure.
5. Defining the boundary conditions.
6. Generating the final mesh, the mesh must be refined around the initial crack and in the regions were the crack expected to grow.
7. Analyzing the results obtained. All analyzed results will be introduced in the following tables and graphs.

4. Results and discussion

All simulation analyzes are performed using ABAQUS/Morfeo software. The calculations obtained including stress intensity factors and crack growth data given as a function of load cycles N and crack length are shown in Table 3, as well as in Figures 4 and 5, respectively

The stiffeners (stringers) indicate redistribute load, and increasing of the structural life of the material welded structure, at the same time stress intensity factors decrease when the crack reaches the stringer compared to unreinforced welded structure. Faster crack growth occurs after load cycles number of cca 70000, as shown in the change of the curve slope in Figure 5. During the propagation of the crack through the structure, change of its direction can be clearly seen after the crack propagation reaches the stringer, it grows vertically within the stringer and horizontally within the base material as it is shown in Figure 4. This is related to shear stresses within the structure leads to two additional fracture modes introduced by their stress intensity factors (K_{II}, K_{III}) Stress intensity factors distribution with crack propagation steps for all modes (Mode I , Mode II , Mode III) can be seen in Table 3. The structure will maintain its integrity since the stress intensity factors is still smaller than the critical stress intensity factors (fracture toughness).

Table 3 Numerical data: stress intensity factors changes with crack growth.

STEP No.	x coord.	y coord.	z coord.	K_{eff}	K_I	K_{II}	K_{III}
STEP 1	32.5	0.416625	84.9999	58.5599	58.5439	1.12209	0.061025
STEP 2	31.501	0.000823	84.9616	70.8492	70.7704	-1.59187	0.017724
STEP 3	30.5011	0.00094	84.9682	82.4329	82.367	0.51373	0.045845
STEP 4	29.5018	0.001465	84.9622	93.7761	93.4894	-0.08391	0.054293
STEP 5	28.5027	0.002259	84.9581	104.499	104.176	0.01841	0.013896
STEP 6	27.5034	0.002846	84.9536	114.94	114.576	0.013571	-0.00807
STEP 7	26.504	0.003378	84.9488	125.261	124.858	0.012528	-0.02873
STEP 8	25.5047	0.003911	84.9439	135.579	135.145	0.008668	-0.03672
STEP 9	24.5052	0.004395	84.9388	146.051	145.593	0.023812	-0.02466
STEP 10	23.5053	0.004428	84.9334	156.409	155.932	0.211431	-0.051
STEP 11	22.5053	0.004479	84.9254	166.581	166.074	0.584981	-0.06266
STEP 12	21.5058	0.004918	84.9104	177.697	177.13	0.681217	-0.01119
STEP 13	20.5089	0.007565	84.8879	189.138	188.523	-0.32102	0.199115
STEP 14	19.5117	0.009874	84.869	202.204	201.587	-0.45661	0.272152
STEP 15	18.5174	0.01481	84.8549	215.592	214.953	-0.18062	0.23008
STEP 16	17.5262	0.022327	84.8428	229.389	228.687	0.013278	0.11272
STEP 17	16.5378	0.032502	84.8312	243.842	243.035	0.048874	0.081264
STEP 18	15.5407	0.035124	84.8194	259.715	258.648	0.184532	0.197215
STEP 19	14.5409	0.035463	84.8073	273.194	271.991	0.657063	0.430872
STEP 20	13.5436	0.037953	84.792	286.13	284.001	1.06159	-2.24119
STEP 21	12.5554	0.04787	84.7723	298.415	295.753	1.66492	-2.17528
STEP 22	11.5614	0.053052	84.7429	310.527	307.224	1.20834	-3.53541

STEP 23	10.5696	0.059875	84.7068	322.066	317.388	1.28617	-5.0629
STEP 24	9.58024	0.069132	84.6635	335.489	329.433	3.80428	-4.43084
STEP 25	8.58906	0.076462	84.5971	351.496	342.527	3.45848	-6.49716
STEP 26	7.60567	0.089946	84.5158	366.723	351.891	3.23582	-9.0617
STEP 27	6.65912	0.008802	84.3886	386.01	361.632	3.12656	10.7498
STEP 28	5.70687	0.390046	84.4829	386.997	347.851	5.99755	-26.5449
STEP 29	4.78826	0.090744	84.2006	384.366	335.805	7.14517	-11.2182
STEP 30	3.86851	0.139307	84.1365	382.047	322.055	9.37619	-11.5448
STEP 31	3.00176	0.000684	83.8674	370.6	298.578	5.2282	5.96545
STEP 32	2.3017	0.004785	83.7541	375.052	301.754	-5.14371	25.9782
STEP 33	1.69232	0.000193	83.6815	368.653	279.84	-19.1624	1.91199
STEP 34	1.20936	-0.0386	83.6885	394.601	331.668	14.5665	25.2557
STEP 35	0.378063	0.05357	83.5783	408.819	347.192	-6.88665	34.5386
STEP 36	-0.77646	-0.41444	83.7738	421.028	377.083	-12.9916	66.6564
STEP 37	-1.53781	0.292509	83.7039	435.628	414.529	-2.07667	34.8246
STEP 38	-2.29268	0.948357	83.6994	437.403	417.769	11.725	7.50726
STEP 39	-2.02817	3.12092	84.0581	461.41	447.037	34.4692	33.2347
STEP 40	-4.90219	-0.9542	83.9546	547.863	494.851	-2.266	68.6755
STEP 41	-5.62922	-1.665	83.1775	613.818	529.835	-67.8504	66.0472
STEP 42	-6.67147	-1.29927	83.7366	670.702	630.018	56.8647	12.69
STEP 43	-7.50136	-2.49964	83.908	756.572	716.132	-23.9424	45.9295
STEP 44	-8.46558	-2.42606	83.9594	764.929	685.254	-169.564	-51.5869
STEP 45	-9.30015	-2.43906	84.4381	772.018	693.016	54.6571	-112.84
STEP 46	-10.1741	-2.43339	84.5713	905.292	811.831	19.779	-149.08
STEP 47	-10.9894	-2.48126	84.7469	991.938	857.934	-35.2377	-171.168

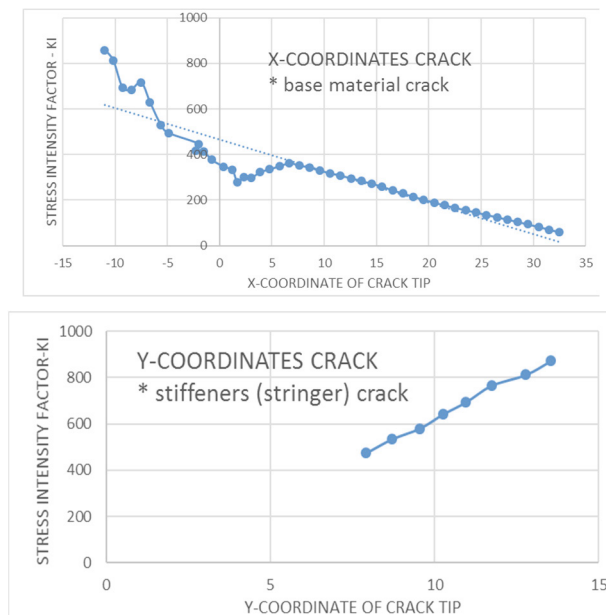


Fig. 4. Stress intensity factors vs x-y coordinates of crack.

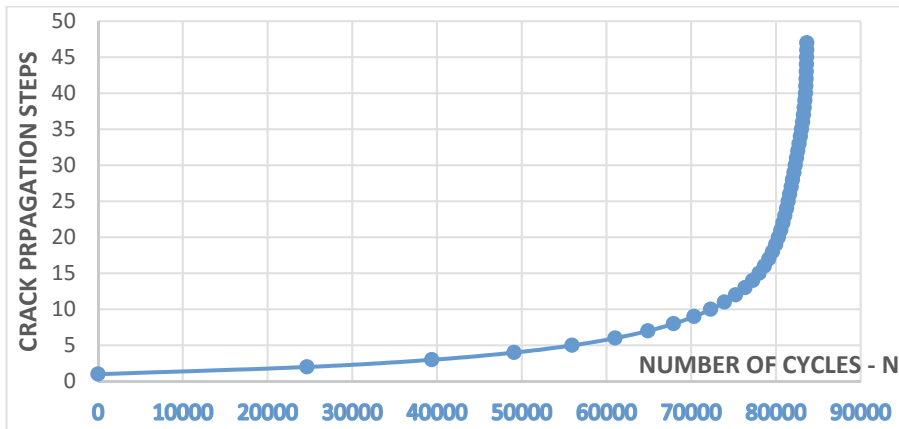
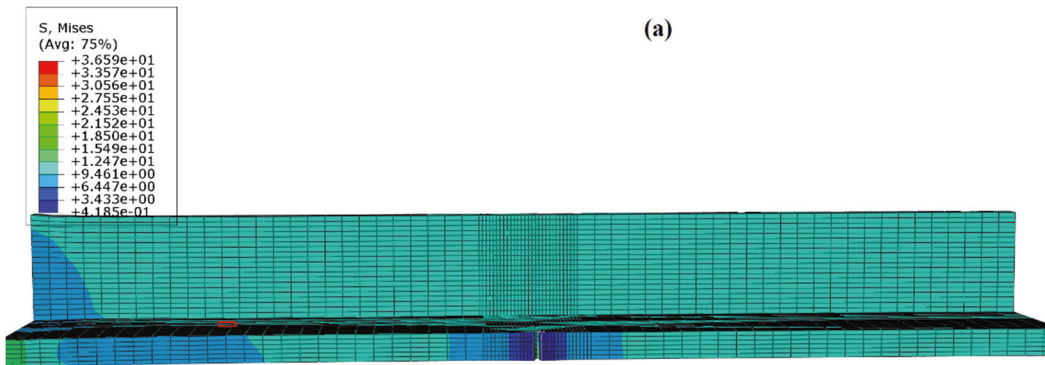


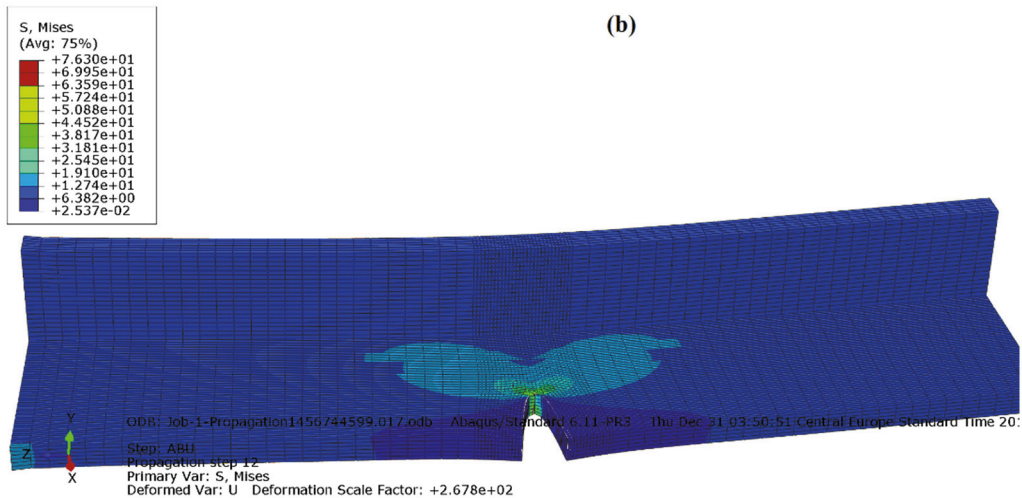
Fig. 5. Number of cycles versus crack propagation steps.

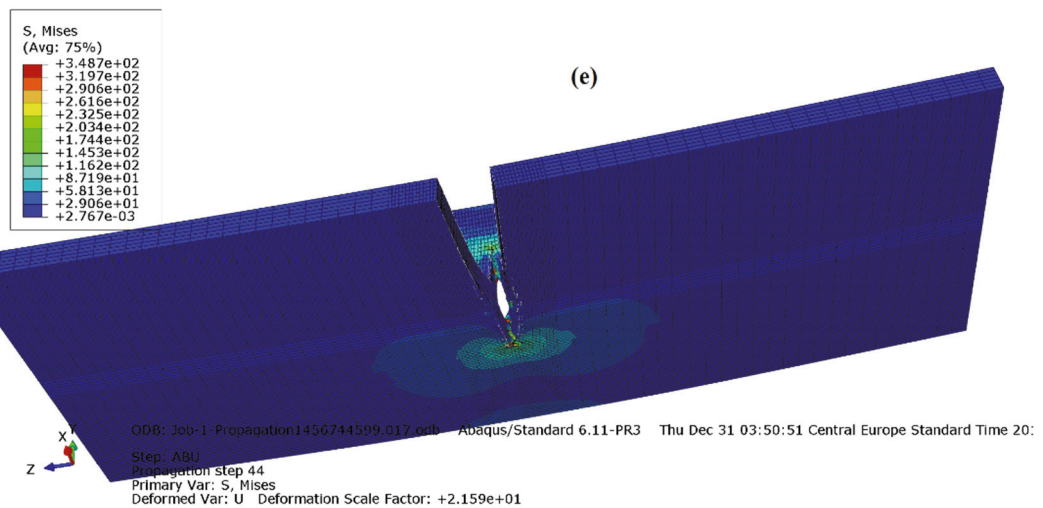
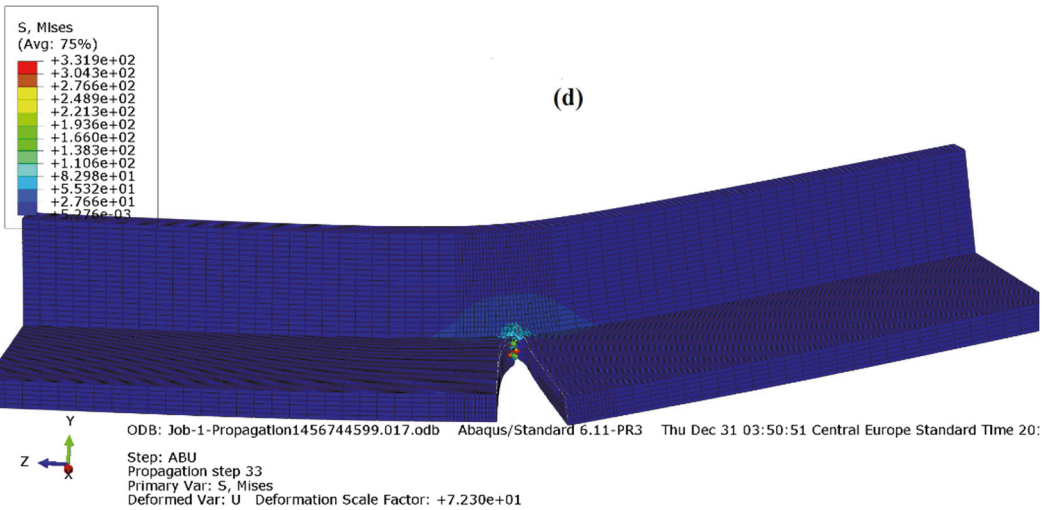
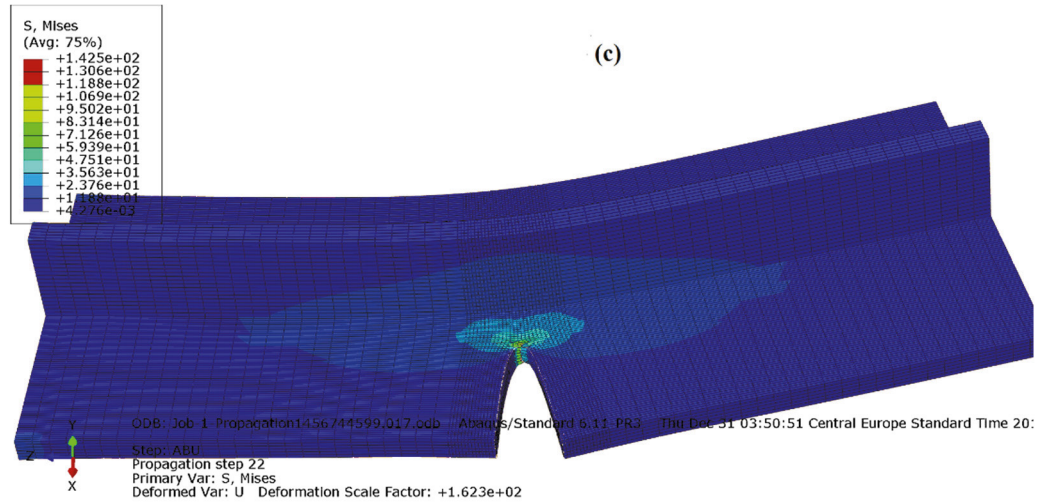
The following illustration is given the distribution of Von Mises stresses in the structure in several steps including step (0) as shown in Figure 6a-f.



Y
Z

ODB: Job-1-Propagation1456744599.017.odb Abaqus/Standard 6.11-PR3 Thu Dec 31 03:50:51 Central Europe Standard Time 20:
Step: ABU
Propagation step 0
Primary Var: S, Mises
Deformed Var: U Deformation Scale Factor: +3.459e+02





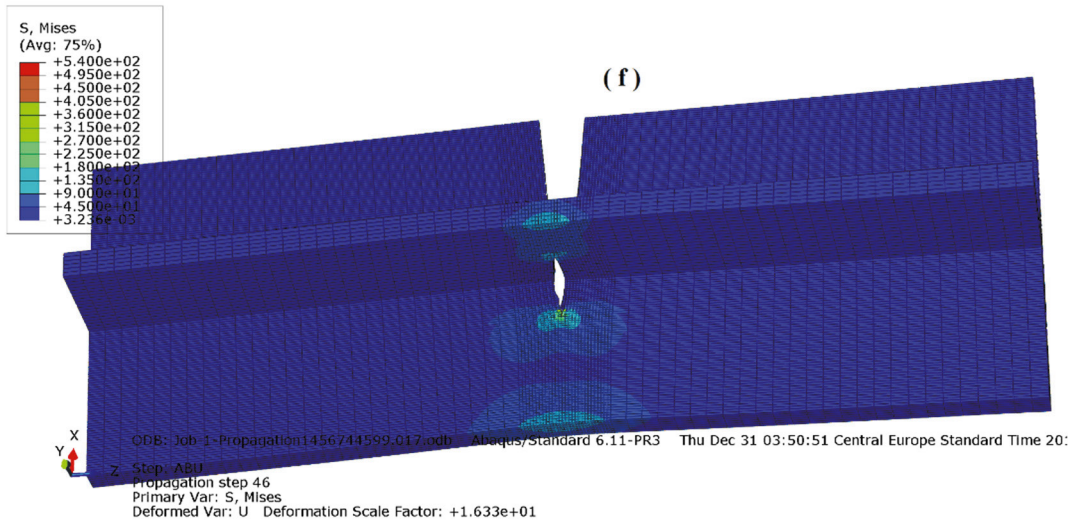


Fig. 6 (a-f). Von Mises stresses for reinforced plate with FSW T-joint. a. Step 0; b. Step 12; c. Step 22; d. Step 33; e. Step 44; f. Step 46.

5. Conclusions

The main results and conclusions of the work presented in this paper are as follows:

- Numerical simulation can be used to determine the right time to withdraw a cracked component from operation, before unstable crack propagation occurs.
- The crack propagates in different directions (base material and stringer) because of shearing stresses in the structure and redistribution of stress intensity factors.

References

- Thomas, W.M., Nicholas, E.D., Needham, J.C., Murch, M.G., Templesmith, P., Dawes, C.J., 1995. Friction Stir Butt Welding, Int.Patent App. PCT/GB92/02203 and GB Patent App. 9125978.8, Dec. 1991. U.S. Patent No. 5,460,317.
- Djordjevic, A., 2015. Friction Stir Welding of Aluminum alloy T joints, (in Serbian) D.Sc. thesis, University of Belgrade, Faculty of Mechanical Engineering.
- Zivkovic, A., Djurdjevic, A., Sedmak, A., Tadic, S., Jovanović, I., Djurdjevic, Dj., Zammit, K., 2015. Friction stir welding of aluminium alloys – t joints, *Structural Integrity and Life* 15(3), 181–186
- Zivkovic, A., Djurdjevic, A., Sedmak, A., Dascau, H., Radisavljevic, I., Djurdjevic, Dj., 2015. Friction Stir Welding of T-joints, Proc. 3rd IIW South-East European Welding Congress, Romania.
- Golestaneh, A. F., Ali, A., Zadeh, M., 2009. Modelling the fatigue crack growth in friction stir welded joint of 2024-T351 Al alloy. *Materials and Design* 30, 2928-2937.
- Golestaneh, A. F., Ali, A., Voon, W. S., Faizal, M., & Mohammadi, M. Z., 2009. Simulation of fatigue crack growth in friction stir welded joints in 2024-T351 Al alloy. *Suranaree Journal of Science and Technology* 16, 35-46.
- Zivojinović, D., Djurdjevic, A., Grbovic, A., Sedmak, A., Rakin, M., 2014. Numerical modelling of crack propagation in friction stir. *Procedia Materials Science* 3, 1330-1335.